



MODELING INHERENT DAMPING IN NONLINEAR DYNAMIC ANALYSIS

F. Charney⁽¹⁾, D. Lopez-Garcia^(2,3), A. Hardyniec⁽⁴⁾, and D. Ugalde⁽⁵⁾

(1) Professor, Virginia Tech, Blacksburg, Virginia, U.S.A. fcharney@vt.edu

(2) Associate Professor, Department of Structural & Geotechnical, Pontificia Universidad Catolica de Chile, dlg@ing.puc.cl

(3) Researcher, National Research Center for Integrated Natural Disaster Management CONICYT/FONDAP/15110017, dlg@ing.puc.cl

(4) Associate, Exponent Failure Analysis Associates, Warrenville, Illinois, U.S.A. ahardyniec@exponent.com

(5) Ph. D. Student, Department of Structural & Geotechnical, Pontificia Universidad Catolica de Chile, dgugalde@uc.cl

Abstract

Modeling of inherent damping in nonlinear dynamic analysis has generated significant interest over the past 35 years, and there is little agreement as to the approach that should be used. In most cases, it is assumed that the damping is linear, viscous, and classical, which is almost universally recognized as unrealistic. Additionally, a host of problems have been identified wherein unrealistic damping forces and other detrimental effects can arise. Methodologies have been forwarded for minimizing or potentially eliminating the problems, but no classical viscous damping model has been developed that is reliable in all circumstances.

In this paper, issues related to modeling damping as linear and viscous are reviewed and explained through the analysis of a simple 4-story moment resisting frame. Approaches evaluated include Rayleigh damping (using full initial stiffness, partial initial stiffness, full tangent stiffness, and partial tangent stiffness), and Modal damping. With regard to tangent stiffness damping, issues related to imparted energy due to negative tangent stiffness, damping force – velocity hysteresis, and implementation with the P-Delta or corotational geometric transformations are discussed. The paper concludes with a recommendation to move away from the use of linear viscous damping, and instead to model inherent energy dissipation as nonlinear, amplitude dependent, frequency independent, and evolutionary.

Keywords: nonlinear dynamic analysis, modeling approaches, damping

1. Introduction

After a structure is put into free vibration, the amplitude of displacement will decay with time. This phenomenon is referred to as damping. Damping also has an effect on forced vibration response, including excitation due to wind and seismic effects. For the purpose of this paper, damping can be characterized in terms of the locations in the building system in which it originates: (1) the lateral load resisting structural systems; (2) the non-lateral load resisting structural systems; (3) the nonstructural/architectural/mechanical system; (4) the underlying soil. In this paper the damping in the soil is not addressed, and the focus is instead on the other three above grade systems.

Within the above grade region of the building system, the principal sources of damping are internal friction in materials and sliding contact among common surfaces. In this paper the sum total of the damping in the three regions specified, due to the sources identified, is referred to as inherent damping. It is important to note that energy dissipated in the inelastic regions of the structural system is not included in inherent damping, as this is treated explicitly in the analysis. Damping due to, say, light cracking in regions of the structure for which the mathematical model remains essentially elastic should be characterized as inherent.

Currently, it is difficult if not impossible to explicitly model the different sources of inherent damping because the nature and the magnitude of the damping cannot be obtained from first principles. Even if the nature of the damping could be identified, the behavior is nonlinear, amplitude dependent, and varies during the response [1]. Due to the difficulty of modeling damping as nonlinear it is almost always represented as linear viscous. Linear viscous damping is frequency dependent and amplitude independent, which is at odds with observed behavior. However, for small damping ratios, and when applied to structures remaining essentially elastic, the linear viscous model is reasonably accurate.

Mathematically, linear viscous damping is quantified by a damping ratio (or damping ratios in different modes) that have been observed from the results of low-amplitude free vibration or modal testing of complete structural systems. The use of viscous damping is almost universal in linear analysis, and for multiple degree-of-freedom systems it is convenient to assume that the damping is classical, allowing decoupling of the system into a number of single degree of freedom systems which can be independently analyzed. For computing inelastic response, damping is usually represented as linear viscous and classical, even though the motivation for such a choice is no longer justified because nonlinear behavior is explicitly considered, and because the equations of motion cannot be uncoupled. In analysis of linear systems, the consequences of assuming linear viscous classical behavior are benign, but in nonlinear analysis severe unintended consequences can occur [2]. In the next section of this paper a theoretical background is provided, which is followed by a discussion of what can go wrong, a description of some of the proposed remedies, an explanation of why some of the remedies produce undesirable side effects, and finally, what might be done to solve the problem.

2. Theoretical Background: Classical Linear Viscous Damping

Over the past 35 years there has been considerable discussion in the technical literature regarding the best approaches for modeling inherent damping in nonlinear dynamic analysis [2-13]. Virtually all of the approaches presented in the literature are based on classical viscous damping, and the principal issues discussed are primarily related to avoiding unintended consequences when classical viscous damping is used.

Two basic approaches are used for developing the damping matrix. In the first approach, the damping matrix has terms associated with only those degrees of freedom that are assigned mass. In the second case the damping matrix has terms that are associated with all degrees of freedom that are assigned stiffness. In this paper the first approach is referred to as *Dynamic DOF Damping*, and the second approach is referred to as *Static DOF Damping*.

2.1 Dynamic DOF Damping

Dynamic DOF Damping, also referred to as Modal Damping, can be traced to Caughey [14], for which the damping matrix, C_c , for an elastic Multiple Degree of Freedom (MDOF) system is expressed as

$$C_c = M \sum_j a_j [M^{-1}K]^j \quad (1)$$

where M is the mass matrix, K is the stiffness matrix, and a_j are coefficients computed from solving the following system of equations:

$$\xi_n = \frac{1}{2} \sum_j a_j \omega_n^{2j-1} \quad (2)$$

In Eq. 2 ξ_n and ω_n are the viscous damping ratios and the associated vibration frequencies. There is no requirement that the frequencies be actual modal frequencies of the system. In Eq. 1 and 2 the index j can take any integer value, and there can be gaps in the sequence. The only restriction is that the number of terms in the summation is equal to the number of frequencies for which associated damping ratios are set. It is common to limit the range of j from 0 to $N-1$, where N is less than or equal to the number of modes in the system (in which case n ranges from 1 to N). It is important to note that when using Eq. 1 and 2 the damping at a given frequency will be zero only if it is set to zero for that frequency.

The system in Eq. 2 becomes difficult to solve for large values of j . Wilson and Penzien [15] provided an alternate procedure for forming the damping matrix that avoids the numerical issues:

$$C_{WP} = M \left[\sum_{n=1}^N \frac{2\xi_n \omega_n}{M_n} \phi_n \phi_n^T \right] M \quad (3)$$

In Eq. 3 M_n is the generalized mass in mode n and ϕ_n is the associated mode shape. The formation of C_{WP} is restricted to frequencies that are natural frequencies of the system. However, there is no requirement that all modes be included, and those modes that are left out will have zero damping.

Before continuing, it is noted that Caughey and Wilson-Penzien damping is “classical”, in that the damping matrix is decoupled when transforming to modal coordinates. Classical behavior does not exist in actual structures, except perhaps under ambient level vibrations in elastic systems [16]. Additionally, it is the loss of classicality when the system yields that presents problems in some of the damping models [5, 13].

A very important feature of Eq. 1 is that the mass matrix M must be invertible, requiring all degrees of freedom to have mass. Thus, for systems with massless DOF, Eq. 1 would be applied to the condensed system. In Eq. 3, it is not strictly required that the mass matrix be invertible, but the number of terms in the summation must be less than or equal to the number of mass degrees of freedom in the system. Given the above, the order of C_c developed from Eq. 1 is $NMDOF$ (the number of mass degrees of freedom), whereas from Eq. 3 the order of C_{WP} is $NDOF$ (the total number of degrees of freedom), unless the equation is applied to the statically system, in which case C_{WP} is identical to C_c . Alternately, C_c could be expanded to the full DOF set, producing a matrix identical to C_{WP} .

A common approach is to apply Eq. 1 with the indices j set to 0 and 1. In this case, the result is

$$C_R = a_0 M + a_1 K \quad (4)$$

where the subscript R indicates that this form of damping is attributed to Rayleigh [17]. The coefficients a_0 and a_1 are easily determined from

$$\begin{Bmatrix} \xi_k \\ \xi_m \end{Bmatrix} = 0.5 \begin{bmatrix} 1/\omega_k & \omega_k \\ 1/\omega_m & \omega_m \end{bmatrix} \begin{Bmatrix} a_0 \\ a_1 \end{Bmatrix} \quad (5)$$

where the damping ratios ξ_k and ξ_m are set at two frequencies ω_k and ω_m , not necessarily natural frequencies of the system. The damping ratio at any other frequency is obtained from Eq. 6:

$$\xi_i = 0.5 \left[\frac{a_0}{\omega_i} + a_1 \omega_i \right] \quad (6)$$

Before discussing the implications of the various forms of damping on inelastic response, it is useful to first examine differences in the damping matrices for elastic systems. If the equations of motion are written for the full system, they can be expressed in partitioned form [13], as follows:

$$\begin{bmatrix} M_{DD} & 0 \\ 0 & 0 \end{bmatrix} \begin{Bmatrix} \ddot{U}_D \\ \ddot{U}_S \end{Bmatrix} + \begin{bmatrix} C_{DD} & C_{DS} \\ C_{SD} & C_{SS} \end{bmatrix} \begin{Bmatrix} \dot{U}_D \\ \dot{U}_S \end{Bmatrix} + \begin{bmatrix} K_{DD} & K_{DS} \\ K_{SD} & K_{SS} \end{bmatrix} \begin{Bmatrix} U_D \\ U_S \end{Bmatrix} = \begin{Bmatrix} P_D(t) \\ 0 \end{Bmatrix} \quad (7)$$

where the subscript *D* represents a Dynamic (mass) DOF, and the subscript *S* represents a Static (massless) DOF. For the Caughey and Wilson-Penzien approaches the damping matrix appears as follows, where the term \hat{K}_{DD} is the statically condensed stiffness matrix.

$$C_C = C_{WP} = \begin{bmatrix} M_{DD} \sum_j a_j [M_{DD}^{-1} \hat{K}_{DD}]^j & 0 \\ 0 & 0 \end{bmatrix} = \begin{bmatrix} \hat{C}_C & 0 \\ 0 & 0 \end{bmatrix} \quad (8)$$

If Caughey damping is used wherein $j=0$ and 1, the damping matrix becomes

$$C_R = \begin{bmatrix} a_0 M_{DD} & 0 \\ 0 & 0 \end{bmatrix} + \begin{bmatrix} a_1 \hat{K}_{DD} & 0 \\ 0 & 0 \end{bmatrix} = \begin{bmatrix} \hat{C}_R & 0 \\ 0 & 0 \end{bmatrix} \quad (9)$$

As discussed later, the forms of the damping matrices given by \hat{C}_C or \hat{C}_R represent a network of virtual viscous dashpots connected between all mass degrees of freedom, and between the masses and virtual supports. There is no damping associated with the structural elements. This idealization has no physical counterpart, but there are certain advantages to avoiding damping in the elements as discussed later. A disadvantage of Eq. 8 and Eq. 9 is that the damping submatrices couple degrees of freedom that are not coupled in the original system, thus the profile of the damping matrix is not the same as that of the stiffness matrix. If it is desired to maintain the profile of the stiffness matrix, iterative procedures have been developed to deal with the damping terms outside the profile [3, 13].

2.2 Static DOF Damping

If the Rayleigh concept is applied to the full system, the damping matrix given by Eq. 10 is obtained, wherein the subscript *RF* refers to Rayleigh damping for the Full system. Here, the mass proportional part of the damping matrix represents virtual dashpots that connect the mass degrees of freedom to virtual external supports, as though the structure were immersed in a viscous fluid. The stiffness part of the damping matrix represents damping in the individual elements, which is physically realistic because damping originates in the elements and the connections.

$$C_{RF} = \begin{bmatrix} a_0 M_{DD} & 0 \\ 0 & 0 \end{bmatrix} + \begin{bmatrix} a_1 K_{DD} & a_1 K_{DS} \\ a_1 K_{SD} & a_1 K_{SS} \end{bmatrix} \quad (10)$$

It is interesting to note, that for elastic systems, analysis using C_R or C_{RF} will produce exactly the same response (including nodal displacements and element elastic forces). If nonlinear analysis is performed using a constant C_{RF} , based on initial system stiffness, the system will become nonclassical as soon as the system stiffness changes, effective damping ratios will increase, and unrealistic damping forces can develop in the elements [2]. While some authors represent these unrealistic element damping forces as “spurious”, or indicate that “unbalanced damping forces” occur, this is technically incorrect. However, the damping forces developed by the $a_0 M_{DD}$ part of the response are spurious, because there is no physical basis for the forces that result from

the “viscous skyhook” nature of the fictitious mass-proportional dashpots. It is for this reason that several researchers [6, 10, 18] have recommended that mass-proportional Rayleigh damping not be used.

An important variation of Rayleigh damping is to use only those terms that remain elastic in the stiffness proportional part of the damping matrix. This approach, which is referred to herein as *Partial Stiffness Proportional Damping* was recommended by Charney [2] and investigated in detail by Zareian and Medina [8]. Use of this damping matrix will eliminate the development of unrealistic damping forces when the system yields, but as noted later, may not eliminate unrealistic damping forces associated with changes in geometry. The mathematical expression for the partial stiffness damping is shown in Eq. 11, where superscript *E* on the stiffness term represents the fact that only those elements that remain elastic during the response are included. In the equation, the proportionality constants are the same as those that would be determined using the full stiffness (Eq. 10). This will result in slightly lower damping ratios than obtained using the full stiffness. For example, for the structure in Fig. 1, the coefficients were determined to produce 5% damping in modes 1 and 3. The damping ratios for all four modes were (0.05, 0.0357, 0.05, 0.658) for an average of 0.0511. If the same coefficients are computed with partial stiffness damping, the ratios in the four modes are (0.049, 0.0323, 0.0429, 0.0572) with an average of 0.050. In this case the difference is negligible, but if desired, the proportionality coefficients could be adjusted by the factor 0.0511/0.050 to obtain an average of 5% damping across the frequency spectrum.

$$C_{RP} = \begin{bmatrix} a_0 M_{DD} & 0 \\ 0 & 0 \end{bmatrix} + \begin{bmatrix} a_1 K_{DD}^E & a_1 K_{DS}^E \\ a_1 K_{SD}^E & a_1 K_{SS}^E \end{bmatrix} \quad (11)$$

2.3 Recovering Damping Ratios after Damping Matrix has been formed

After the damping matrix is established, it is useful to recover the damping ratios in the different modes of the system. The most general approach, which is exact for both classically and nonclassically damped systems is to compute the eigenvalues of the state space matrix *D*, shown in Eq. 12, where [*I*] is an identity matrix and [0] is a zero matrix [19]. The eigenvalues for subcritical modes are complex (even for classically damped systems), and contain the damping ratio and the frequency of the mode. For damping less than critical the eigenvalues are complex numbers of the form *Re+Im*i*. The eigenvectors are also complex, where each coordinate of each vector (mode shape) contains both amplitude and phase. The frequencies in each mode are found as $\omega = \sqrt{Im^2 + Re^2}$ and the damping ratios are $\xi = -Re/\omega$.

$$D = \begin{bmatrix} -M^{-1}C & -M^{-1}K \\ [I] & [0] \end{bmatrix} \quad (12)$$

A limitation on the use of Eq. 12 is that the mass matrix must be nonsingular. Thus, for Dynamic DOF Damping the matrices *M* and *C* in Eq. 12 will be the appropriate submatrices shown in Eq. 8.

An approach that is useful when the mass matrix is not invertible is to compute the modal damping ratios as in Eq. 13, where ω_i is the circular frequency and ϕ_i is the mode shape for mode *i* of the complete system. This approach is exact for classically damped systems, and is approximate for nonclassically damped systems. It is useful for computing the modal damping in systems with Static DOF damping because the mass matrix for these systems is generally singular.

$$\xi_i = \frac{\phi_i^T C \phi_i}{2\omega_i \phi_i^T M \phi_i} \quad (13)$$

2.4 Arrangement of Fictitious Viscous Dashpots

Consider the structure of Fig. 1 which is analyzed throughout the remainder of this paper. The structure is a four-story one-bay moment resisting frame. All of the mass for the system is concentrated at the midspan of the beams, and is active only in the global *X* direction, and hence, the system has only four mass degrees of freedom.

Inelastic behavior is lumped into “plastic hinges” near the ends of the beams and columns. All frame elements are flexible axially and in bending, and as modeled there are a total of 132 degrees of freedom.

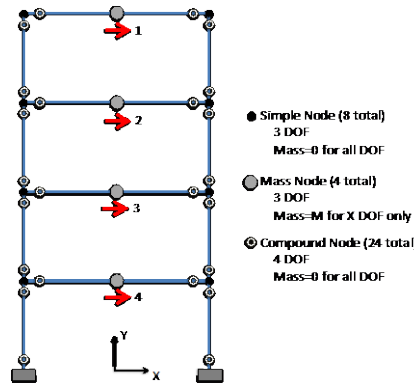


Fig. 1 - 4-Story Moment Frame Used in Analysis

Where Caughey damping is used, the damping submatrix \hat{C}_C (Eq. 8) has four rows and four columns, and is usually full. The fullness of the matrix represents a physical 4-story shear-frame with only lateral DOF in which viscous dashpots connect all possible combinations of degrees of freedom as shown in Fig. 2a. Off diagonal terms can be either positive or negative, and where positive, the damping constant for the associated dashpot is negative. In the figure three types of dashpots are represented: those that connect adjacent stories (green), those that connect non adjacent stories (blue), and those that connect stories to the base or to external supports (red). The dampers at each level that are attached to external supports are effectively mass proportional. This component of damping cannot be eliminated and can be problematic when analyzing certain types of structures, such as seismically isolated systems [6,18]. Where Caughey-Rayleigh Damping is used the arrangement of dashpots is the same as in Fig. 2a. However, in this case the mass proportional dampers can be eliminated by setting a_0 equal to zero. This will lead to damping ratios that increase linearly with frequency.

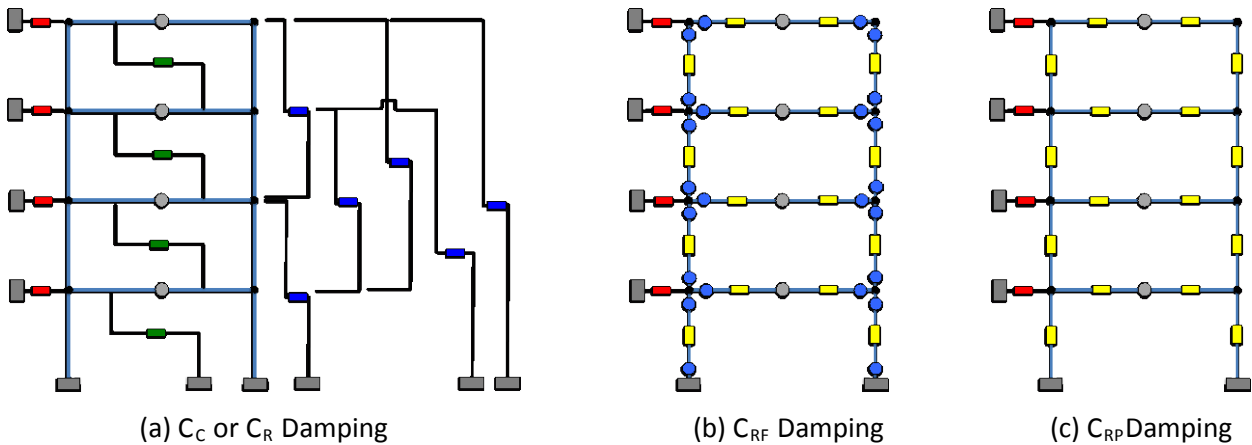


Fig. 2 Arrangement of Virtual Viscous Dashpots in Various Damping Models

From a viscous damping perspective, there is clearly no physical basis for the arrangement of dashpots in Fig. 2a, except that it is required to provide classical damping in the elastic system. When the system yields, this same arrangement of dashpots is maintained, and the effect on the nonlinear response is difficult to predict.

When the damping matrix is established as in Eq. 10, the arrangement of fictitious dashpots is as shown in Fig. 2b. Here, the mass proportional dashpots remain (if a_0 is not equal to zero), but the remaining dashpots are attached to the elements as visualized in the figure. Note that the yellow rectangles represent damping proportional to the element stiffness matrix, and the blue circles represent damping proportional to the stiffness of the rotational springs used to represent inelastic behavior. The elimination of these (blue) rotational dampers produces the variation of stiffness proportional damping called Partial Initial Stiffness Proportional Damping

herein. This is illustrated in Fig. 2c. To the authors, in spite of the presence of the mass proportional dashpots, this is a much more reasonable arrangement of damping in the system because damping is generated within the elements, not in fictitious viscous dashpots.

3. What Can go Wrong (Will go Wrong)

A large number of papers have been published on what can go wrong when damping is modeled as linear viscous and classical in nonlinear dynamic analysis. Some of these issues were recognized in the thesis by Chrisp [3], and discussed in more detail (for example) by Bernal [5], Hall [6], and Charney [2]. It is noted that none of the issues reported deal with the fundamental problem that linear viscous classical damping is inherently incorrect (e.g. actual damping is displacement dependent and viscous damping is not). Instead, the issues are related to unintended consequences of modeling damping as linear viscous, and in most cases, the problem is the development of unrealistic damping forces when the system yields, transforming the system from classical to nonclassical. A few of the problems, proposed remedies, and unresolved issues with potentially adverse side effects of the remedies are presented in the following.

3.1 The Influence of Global Changes in System Stiffness on Instantaneous Damping Ratios

Here the issue is that changes occur in the damping ratios when the damping matrix is based on the initial stiffness and held constant, and then the stiffness changes due to yielding in the plastic hinges. To illustrate this effect analysis was performed on the system shown in Fig. 1 using Rayleigh damping set to 2% critical in modes 1 and 3, and with Modal damping set to 2% in all modes. Yielding in the hinges was represented by reducing the stiffness from $EI/20$ to $EI/1000$, where EI is the beam stiffness. Note the stiffness of $EI/20$ is approximately the smallest order of magnitude value at which the hinge is effectively rigid prior to yielding. The following variations in the system were analyzed:

Model O: Original System

Model A: Reduction in hinge stiffness at top and bottom of lower story columns (column sway mechanism)

Model B: Reduction in stiffness in hinges at ends of all beams

Model C: Reduction in stiffness in hinges in bottom of first story columns at ends of all beam hinges (system sidesway mechanism)

For each model the frequencies and damping ratios of the modified system were determined by computing the eigenvalues of the system's state space matrix (Eq.12). Results from the analysis are presented in Table 1 where it can be seen that the damping ratios in the first mode of the damaged system increase significantly for both Rayleigh and Modal damping. For model C, which represents a sidesway collapse mechanism, the damping increases from 0.02 to 0.068 in the first mode, representing an increase by a factor of 3.4. While not included in the analyses reported here, similar changes in modal damping ratios will occur when the damping is proportional to the partial initial stiffness (Eq. 11).

Table 1 - Changes in damping ratios for damaged system

Frequency/ Damping Ratio	Dynamic DOF Rayleigh Damping				Dynamic DOF Modal Damping			
	O	A	B	C	O	A	B	C
ω_1 (rad/sec)	9.91	4.85	4.33	2.94	9.91	4.84	4.33	2.94
ξ_1	0.020	0.055	0.047	0.068	0.020	0.057	0.047	0.068
ξ_2	0.014	0.028	0.025	0.030	0.020	0.033	0.034	0.042
ξ_3	0.020	0.024	0.025	0.028	0.020	0.024	0.025	0.028
ξ_4	0.026	0.027	0.027	0.029	0.020	0.021	0.021	0.022

Whether or not the increases in system damping are problematic depends on the system being analyzed. For reinforced concrete structures, for example, cracking will develop in the "elastic" region of the elements, and this cracking will progressively increase the material damping in the system. Such increases in damping have been observed in field tests [1]. The problem is not so much that the increase in damping is not realistic, but rather that it is not easily predicted, and if predicted, there is little basis for determining if the increases are excessive.

3.2 Inelastic Behavior in Individual Components

A more serious issue than reported above is the development of large unrealistic damping forces in the inelastic elements when the damping is based on the full initial stiffness (Eq. 10). The best example of this problem is when a phenomenological plastic hinge with high initial stiffness yields. After yielding there is a spike in rotational velocity within the hinge, and this velocity, multiplied by the high initial stiffness and by the stiffness proportionality factor a_1 produces viscous moments that can easily exceed the true flexural capacity of the hinge. This effect can be minimized by using a lower initial stiffness of the hinge [2, 13], or by use of distributed plasticity (fiber) elements [13]. Two other approaches are more common. The first approach is to form the stiffness proportional part of the damping matrix by assembling only the elastic parts of the structure (Eq. 11). This is the Partial Initial Stiffness Damping method described earlier. The second approach is to populate the stiffness proportional part of the damping matrix with the instantaneous tangent stiffness of all elements, including the yielding components. This approach is referred to as Tangent Stiffness Damping.

Usually, with Tangent Stiffness damping, the proportionality constants a_0 and a_1 are based on the initial stiffness and are not updated. In a more refined approach the coefficients are updated but this is rarely used due to the perceived need to re-compute the system frequencies at each change in stiffness. The use of Tangent Stiffness damping will eliminate the unrealistic damping forces, and will minimize the increase in the system damping ratios discussed above. However, there are two concerns that have been raised. The first is that with tangent stiffness damping “hysteresis” develops in the damping-force versus deformational velocity relationship and that there is no physical basis for this phenomenon. Second, where the element tangent stiffness is negative, there is concern that energy may be imparted into the system, rather than dissipated. These issues are explored briefly in this paper.

Where Partial Initial Stiffness damping is used, the unrealistic damping forces in the yielding components cannot form as there is no damping associated with these components. However, in research reported by Hardyniec [20], it has been noted that the combination of Partial Initial Stiffness damping and the use of the corotational transformation in OpenSEES [21] to represent geometric nonlinearities can produce unrealistic damping forces in the elastic elements. As demonstrated later in this paper, this problem can be avoided by using instead the P-Delta geometric transformation, or by using Partial Tangent Stiffness damping.

3.2.1 Issues Related to Full Tangent Stiffness Damping

3.2.1.1 Hysteresis in Force-Velocity Relationship

The issue of hysteresis in the Force-Velocity relationship for tangent stiffness proportional elements was raised by Carr [22], and mentioned more recently by Chopra and McKenna [13]. For traditional structural systems there is no physical analog for this behavior, which is illustrated in Fig. 3 for a bilinear system with positive post-yield stiffness, and in Fig. 4 for a bilinear system with negative post-yield stiffness. In both cases the response is due to a ramped up sinusoidal rotation in a plastic hinge. The computed moment vs. rotation relationship for the spring is shown on the left of each figure, the viscous moment vs. rotational velocity in the center, and the viscous moment vs. rotation is at the right. The units of the enclosed portion of the viscous moment vs. rotational velocity plots are in.-k/second, which is a unit of power. A physical analog would of an active control system that is imparting a changing moment into the system. This in fact would need to be done to keep the damping constant, as is effectively the goal in tangent stiffness damping. As can be seen by comparing the center portions of Fig. 3 and 4, the areas within the enclosed regions of the viscous moment vs. rotational velocity plot is increased when the tangent stiffness is negative. The issue is indeed troubling, and adds one more item of concern to the growing list of discrepancies between classical viscous damping and reality.

The third part of Fig. 3 and 4 shows the viscous moment vs. rotation relationship for the hinge with positive or negative secondary stiffness, respectively. Comparing the regions of the figure enclosed by the dotted line, it can be seen that the system with negative tangent stiffness is producing instantaneous negative energy, but this is small compared to the total energy dissipated by the hinge.

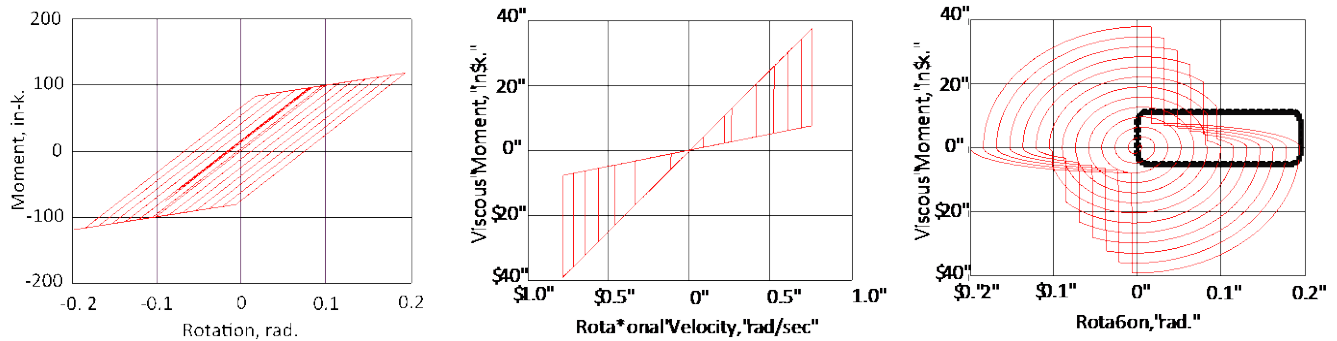


Fig. 3– Computed Behavior with Positive Tangent Stiffness

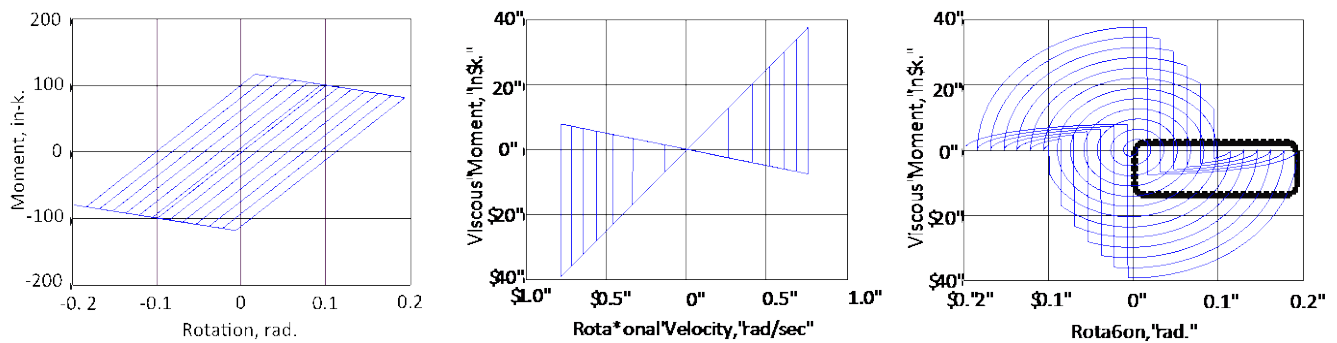


Fig. 4 – Computed Behavior with Negative Tangent Stiffness

3.2.1.2 Negative Tangent Stiffness

Among all the articles reviewed by the authors of this paper, none specifically investigated the impact of negative tangent stiffness where tangent stiffness proportional damping is used. Charney [2] recommended that geometric stiffness not be included in the stiffness proportional part of the damping matrix to avoid issues related to the global tangent stiffness being negative. However, the models used in the reported analysis [2] had bilinear force-deformation relationships with zero strain hardening. Hardyniec and Charney [12] and Chopra and McKenna [13] indicated that negative tangent stiffness was problematic, but did not pursue the matter.

To further investigate this issue, an Incremental Dynamic Analysis (IDA) was performed on the structure shown in Fig. 1, subjected to the East-West component of the Tabas Dayhook ground motion, initially scaled to have a peak ground acceleration of 0.75g. Analysis was run using the following damping models: Full Initial Stiffness, Full Tangent Stiffness, Partial Initial Stiffness, and Partial Tangent Stiffness. Using these damping models three different strain hardening ratios (relative to the initial stiffness) were used: positive 0.02, zero, and negative 0.02. The results for the negative strain hardening ratios are shown in Fig. 5, with each plot showing the computed IDA curves for a single damping ratio, and for the four different models.

As may be observed from Fig. 5, the Full Initial Stiffness damping model produces the greatest apparent collapse capacity for each of the damping ratios, this being due to artificial damping occurring in the hinges. Higher damping ratios and higher initial stiffness causes more significant artificial damping. The results for Partial Initial Stiffness and Partial Tangent Stiffness damping should be identical for each damping ratio, and this is indeed the case because the yielding components are excluded from the model. What is most interesting is that there is very little difference between the results computed using Partial Initial Stiffness damping and Tangent Stiffness damping, even for damping ratios of 0.08. Apparently the “imparted energy” issue is having a negligible influence on the computed response, because if it were having an influence the IDA curve for Tangent Stiffness damping would be below the curve for Partial Initial Stiffness Damping. It is important to note,

however, that more analyses needs to be performed on systems with negative tangent stiffness before an overall conclusion can be made.

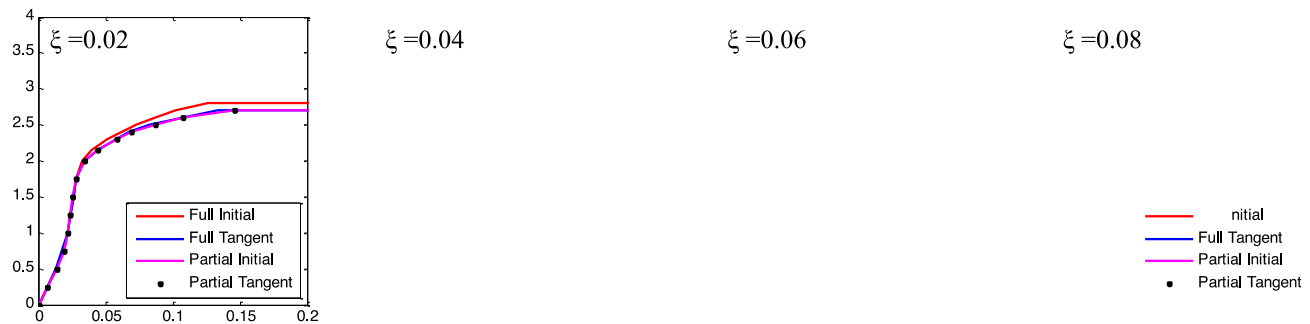


Fig. 5 – IDA Plots for Different Damping Models and Damping Ratios (-2% Strain Hardening)

Another issue regarding negative tangent stiffness is that this will not always occur for design-based analysis performed under the requirements of ASCE 7-16 [23]. Global acceptance criteria for drift in ASCE 7 is that the median story drift at the edge of the building, among eleven required ground motions, shall not exceed $2.0/I_e$ times the story drift limits in Chapter 12, where I_e is the importance factor. For most buildings, the story drift limits would be 0.04, 0.032, and 0.027 for Risk Categories II, III, and IV, respectively. The structural component deformation acceptance criterion in ASCE 7 is tied to the ASCE 41-13 [24] requirements for Primary Components at the Collapse Prevention limit state (also modified by I_e). Under these drift and deformation limits it is unlikely that many components would have inelastic excursions to the extent that the tangent stiffness is negative, and if this occurred, it would occur only in a limited number of elements.

Thus, in summary regarding the use of Tangent Stiffness Damping, there is legitimate concern that the hysteresis in the damping force vs. velocity relationship is occurring and has no physical basis. Regarding energy being imparted into the system, this does appear to occur, but the influence on performance appears to be negligible. It is recommended, however, that this issue be carefully monitored where Full Tangent Stiffness damping is used, particularly in assessing the collapse performance of buildings.

3.2.2 Issues Related to Partial Initial Stiffness Damping and Changes in Geometry

In Partial Initial Stiffness Damping no stiffness proportional damping is assigned to elements that may yield during response. This type of damping completely eliminates the unrealistic viscous forces that develop due to sudden changes in rotational velocity when the elements transition from elastic to inelastic. The larger the initial stiffness of the yielding components, the larger the viscous force [2,13]. In research performed by Hardyniec [20, 25] it was shown that unrealistic damping forces can also occur due to sudden changes in geometry when Partial Initial Stiffness damping is used in association with the corotational transformation in Open Sees. The artificial damping forces are minimal where the P-Delta transformation is used in lieu of the corotational transformation. For both types of geometric transformation the artificial damping forces are eliminated when Partial Tangent Stiffness damping is used.

This behavior is shown in Fig. 6 which are roof displacement histories of a 4-story steel frame. In part (a) of the figure the P-Delta transformation was used, and in part (b) the corotational transformation was utilized. In each case analysis was run using Partial Initial Stiffness damping (KO), and Partial Tangent Stiffness damping (KT). Also varied was the cross sectional area of the modeled beams, where the term Area in the figures represents a *multiplier* on the actual cross sectional area. This type of multiplier is often used to represent rigid diaphragm behavior in 2-D frame analysis. As seen in part (a) of Fig. 6 the responses are similar for all variations in analysis and modeling parameters, and the collapse of the system is captured reasonably well. On the otherhand, in Fig. 6 (b), the collapse is suppressed due to artificial damping forces being developed in the beams when Partial Initial Stiffness damping is used. When this is changed to Partial Tangent Stiffness damping, the correct response is obtained. Although the issues regarding the use of the corotational geometric

transformation can be avoided by use of Partial Tangent Stiffness damping, the broader issue is why changes in geometry should affect system damping at all.

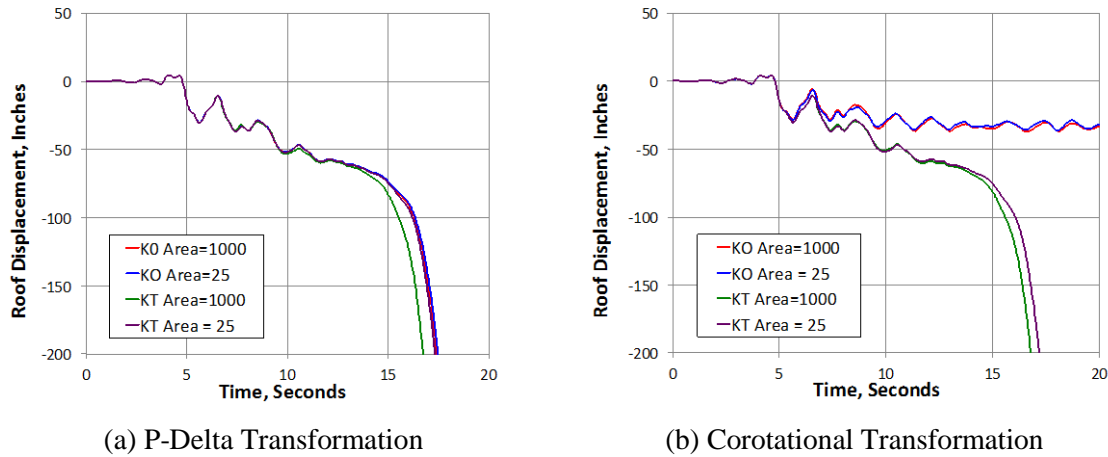


Fig. 6 - Results of Analysis Produced using Partial Initial and Partial Tangent Stiffness Damping and two Methods for Representing Geometric Nonlinearity

4. Summary, Conclusions, and Recommendations

There are many choices available to the analyst for modeling damping in nonlinear response history analysis. These methods can be divided into two groups: Dynamic DOF approaches, wherein the damping matrix is based on the DOFs that have participating mass, and Static DOF approaches, where the damping matrix is based on the full DOF set. While the analyst has more control on setting damping ratios with Dynamic DOF damping, it is generally not possible to eliminate the mass proportional terms. Another disadvantage of Dynamic DOF damping is the need to “right hand side” damping terms that are outside the elastic stiffness profile, and iterate to obtain equilibrium, even for elastic systems. The principal advantage of Dynamic DOF damping is that unrealistic damping forces will not occur when the system yields.

In Full Initial Stiffness damping, which is a Static DOF procedure, it has been demonstrated that unrealistic damping forces can be generated when the system yields. Two basic approaches have been proposed to eliminate this problem: Full Tangent Stiffness damping, and Partial Initial Stiffness damping. Full Tangent stiffness damping, although effective in limiting the unrealistic damping forces, is conceptually flawed due to “hysteresis” being developed in the damping force versus velocity relationships of the yielding elements. While the flaw is troubling, there is currently no evidence that it leads to unrealistic computed response. Another issue with tangent stiffness damping is the potential for energy to be imparted into the system when the instantaneous tangent stiffness of yielding elements is negative. It appears, however, that the influence of imparted energy on the computed response is minimal. Additionally, imparted energy is not expected to be an issue for design-based analysis because the generally conservative deformation-based acceptance criteria makes it highly unlikely that inelastic deformations will be of sufficient magnitude to produce negative tangent stiffness in more than just a few elements at one time.

The use of Partial Initial Stiffness damping eliminates all spurious damping associated with material inelastic behavior, but can produce large unrealistic damping forces when the corotational transformation is used to account for changes in geometry. Where collapse analysis is being performed and it is deemed necessary to use the corotational transformation, Partial Tangent Stiffness damping should be used.

For design-based analysis, it is recommended that Partial Initial Stiffness damping be used, with geometric stiffness excluded from the stiffness proportional part of the damping matrix. Additionally, consideration should be given to minimizing or eliminating the mass proportional part of the damping, as this is physically unrealistic. Elimination of mass proportional damping has the influence of producing higher damping in higher modes, but there is evidence that this behavior is realistic [1].

What should be clear from the host of issues associated with the use of classical viscous damping in nonlinear analysis is that a new approach needs to be developed that treats inherent damping as a nonlinear deformation-dependent and evolutionary path-dependent phenomenon. Such procedures have been suggested in [9, 22, and 26], and these should be pursued by researchers instead of continuing down the path of finding remedies for the unintended consequences of using classical viscous damping.

5. References

- [1] Spence, S M J, and Kareem, A (2014): Tall buildings and damping: A concept-based data-driven model, *Journal of Structural Engineering*, 140(5).
- [2] Charney F A (2008): Unintended consequences of modeling damping in structures, *Journal of Structural Engineering*, 2008:581-592.
- [3] Chrisp D (1980): Damping models for inelastic structures, Master's Thesis, University of Canterbury, Christchurch New Zealand.
- [4] Leger P, and Dussault S (1992): Seismic energy dissipation in MDOF structures, *Journal of Structural Engineering*, 118:1251-1269.
- [5] Bernal D (1994): Viscous damping in inelastic structural response, *Journal of Structural Engineering*, 120:1240-1254.
- [6] Hall J F (2006): Problems encountered from the use (or misuse) of Rayleigh damping, *Earthquake Engineering and Structural Dynamics*, 35:525-545.
- [7] Petrini L, Maggi C, Priestly M J N, and Calvi M G (2008): Experimental Verification of Viscous Damping Modeling for Inelastic Time History Analysis, *Journal of Earthquake Engineering*, 12(S1):125-145.
- [8] Zareian, D and Medina R A (2010): A practical method for proper modeling of structural damping in elastic plane structural systems, *Computers and Structures*, 88:45-53.
- [9] Puthanpurayil A M, Dhakal R P, and Carr A J (2011): Modelling on in-structure damping: a review of the state-of-the-art, *Proceedings of the Ninth Pacific Conference on Earthquake Engineering*, Auckland, New Zealand.
- [10] Smyrou E, Priestly MJN, Carr A (2011): Modeling of Elastic Damping in Nonlinear Response History Analysis of Cantilever RC Walls, *Bulletin of Earthquake Engineering*, 9:1559-1578.
- [11] Jehel P, Leger P L, and Ibrahimbegovic A (2013): Initial vs. tangent-stiffness based Rayleigh damping in inelastic time history analysis, *Earthquake Engineering and Structural Dynamics*, 00:1-16.
- [12] Hardyniec A and Charney F (2015): An investigation into the effects of damping and nonlinear geometry models in earthquake engineering analysis, *Earthquake Engineering and Structural Dynamics*, 44:2695-2715.
- [13] Chopra A K and McKenna F (2016): Modeling viscous damping in nonlinear response history analysis of buildings for earthquake excitation, *Earthquake Engineering and Structural Dynamics*, 42:193-211.
- [14] Caughey T K (1960): Classical normal modes in damped liner systems, *Journal of Applied Mechanics*, 27:269-271.
- [15] Wilson, E, and Penzien, J (1972): Evaluation of orthogonal damping matrices, *International Journal of Numerical Methods in Engineering*, 4:5-10.
- [16] Adhahari S, and Woodhouse J (2001): Identification of damping: Part 1, Viscous damping, *Journal of Sound and Vibration*, 243(1):43-61.
- [17] Rayleigh L. (1045): *Theory of Sound*, vol 1. Dover: New York, N.Y.
- [18] Ryan K L and Polanco J (2008): Problems with Rayleigh Damping in Base Isolated Buildings, *Journal of Structural Engineering*, 134:1780-1784.
- [19] Liang Z and Lee G C (1991): Damping of Structures: Part 1 Theory of Complex Damping, Report NCEER 91-0004, National Center for Earthquake Engineering Research, University of Buffalo, Buffalo, N.Y.
- [20] Hardyniec A (2014): An Investigation of the Behavior of Structural Systems with Modeling Uncertainties, Ph.D. Dissertation, Department of Civil and Environmental Engineering, Virginia Tech, Blacksburg, VA.
- [21] Pacific Earthquake Engineering Research Center (PEER) (2015). Open Systems for Earthquake Engineering Simulation (OpenSees), version 2.4.6. PEER, University of California, Berkeley, California.
- [22] Carr A (2007): *Ruamoko Manual*, University of Canterbury, Christchurch, New Zealand.
- [23] ASCE 7-16 (2016): Minimum Design Loads and Associated Criteria for Buildings and Other Structures, American Society of Civil Engineers, Reston, VA.
- [24] ASCE 41-13 (2014): *Seismic Evaluation and Retrofit of Existing Buildings*, American Society of Civil Engineers, Reston, VA.
- [25] Hardyniec A, and Charney, F (2016): Response to Professor John Hall's discussion of Hardyniec and Charney's paper 'An Investigation into the effects of damping and nonlinear geometry models in earthquake engineering analysis', *Earthquake Engineering and Structural Dynamics*, DOI: 10.1002/eqe.2788.
- [26] Bowland, A., Charney F, Moen C D, and Jarrett J (2010): New Concepts in Modeling Damping in Structures, *Proceedings of the 9th National and 10th Canadian Conference in Earthquake Engineering*, Toronto.